

UDC 004.93

D. Koshutina

Odessa Polytechnic National University, Shevchenko Ave. 1, Odesa, Ukraine, 65044, e-mail: d.v.koshutina@op.edu.ua

KAN-TYPE NEURAL NETWORK MODEL FOR ECG SIGNAL ANALYSIS AND CLASSIFICATION

Д. Кошутіна. **Нейромережева модель KAN-типу для аналізу та класифікації сигналів ЕКГ.** Дослідження електрокардіограм має критичне значення для діагностики серцево-судинних патологій, оскільки точне виділення локальних особливостей сигналу забезпечує надійність класифікації аритмій. Актуальність роботи обумовлена потребою підвищення точності автоматизованих систем, здатних працювати із сегментами сигналів різної довжини та в умовах шумового впливу. Метою роботи є розробка моделі на основі багатощарового перцептрона з додатковим шаром, що комбінує радіальні базисні функції та вейвлет-перетворення для точного виявлення локальних особливостей сигналу. Завдання включали підготовку та нормалізацію сегментів сигналів, експериментальне порівняння різних типів вейвлетів і рівнів їх декомпозиції, вибір числа функцій у додатковому шарі та оцінку впливу архітектурних параметрів на точність класифікації та швидкодію моделей. Методи дослідження передбачали обробку сигналів із відкритої бази даних, нормалізацію значень сегментів у визначеному діапазоні, побудову моделей із застосуванням багатокласової функції втрат і методів оптимізації градієнтного спуску, а також оцінку ефективності через точність класифікації і показники збалансованої точності для сегментів зі шлуночковими порушеннями ритму. Результати показали, що інтеграція додаткового шару з радіальними базисними функціями і вейвлет-перетворенням підвищує точність класифікації аритмій, забезпечує стабільність моделей при зміні параметрів сегментації та наявності шуму, а також дозволяє ефективно виділяти локальні особливості сигналу. Застосування різних типів вейвлетів і рівнів декомпозиції дозволяє досягти оптимального співвідношення точності та швидкодії моделей. Наукова новизна полягає у поєднанні радіальних базисних функцій із вейвлет-перетворенням для покращеного виділення локальних ознак сигналів електрокардіограми, що забезпечує підвищену стійкість до шуму. Практичне значення роботи полягає у створенні ефективної методики для автоматизованого аналізу електрокардіограм із високою точністю класифікації аритмій.

Ключові слова: електрокардіограма, багатощаровий перцептрон, MLP-KAN, вейвлет-перетворення, радіальні базисні функції, класифікація, точність

D. Koshutina. **KAN-Type Neural Network Model for ECG Signal Analysis and Classification.** Electrocardiogram analysis is critically important for the diagnosis of cardiovascular pathologies, as precise identification of local signal features ensures reliable arrhythmia classification. The relevance of this work is determined by the need to improve the accuracy of automated systems capable of processing signal segments of varying length under noisy conditions. The objective of the study is the development of a model based on a multilayer perceptron with an additional layer that combines radial basis functions and wavelet transformation for accurate detection of local signal characteristics. The tasks included preparation and normalization of signal segments, experimental comparison of different types of wavelets and their decomposition levels, selection of the number of functions in the additional layer, and assessment of the impact of architectural parameters on classification accuracy and computational performance. The research methods involved processing signals from an open database, normalizing segment values within a defined range, constructing models using a multiclass loss function and gradient descent optimization, and evaluating performance through classification accuracy and balanced accuracy metrics for segments with ventricular rhythm disturbances. The results demonstrated that integrating an additional layer with radial basis functions and wavelet transformation increases arrhythmia classification accuracy, ensures model stability under variations in segmentation parameters and noise presence, and allows effective extraction of local signal features. The use of different wavelet types and decomposition levels enables achieving an optimal balance between accuracy and computational efficiency. The scientific novelty lies in combining radial basis functions with wavelet transformation to enhance the detection of local electrocardiogram signal features, providing increased noise robustness. The practical significance of the study is the creation of an effective methodology for automated electrocardiogram analysis with high arrhythmia classification accuracy.

Keywords: electrocardiogram, multilayer perceptron, MLP-KAN, additional layer, wavelet transformation, radial basis functions, classification, accuracy

1. Introduction

Electrocardiographic (ECG) signals are a primary diagnostic tool for monitoring cardiac activity and detecting rhythm disturbances. Accurate analysis of ECG signals is crucial for early identification of cardiovascular pathologies, as subtle variations in wave morphology can indicate serious conditions [1]. Traditional signal processing techniques, such as digital filtering, morphological feature extraction, and R-peak detection algorithms – including the Pan-Tompkins approach and wavelet transforms – have provided reliable tools for feature extraction; however, their performance heavily depends on preprocessing quality and careful parameter tuning [1].

The rise of high-performance computing has enabled the adoption of machine learning methods, such as support vector machines, decision trees, and ensemble models, which allow partial automation of feature extraction. Yet, these models often struggle to capture the complex nonlinear dependencies and inter-patient variability inherent in ECG signals [2]. Recent developments in deep learning, in-

DOI: 10.15276/opu.2.72.2025.17

© 2025 The Authors. This is an open access article under the CC BY license (<http://creativecommons.org/licenses/by/4.0/>).

cluding convolutional, recurrent, and hybrid architectures, have demonstrated remarkable performance in ECG classification tasks [3]. Despite these advances, classical multilayer perceptron (MLP) models and their extensions remain relevant due to their structural simplicity, stability during training, and precise control over architectural parameters.

An emerging approach involves Knowledge-Augmented Networks (KAN), which integrate MLP architectures with radial basis functions (RBFs) to enhance the network's ability to approximate local signal features [4]. Such models generate localized responses to morphological variations, improving detection of pathological contractions while preserving overall network stability.

The present study aims to investigate the effectiveness of a KAN-type neural network for ECG classification, comparing it to conventional MLP models. The research focuses on analyzing the impact of RBF components and wavelet-based preprocessing on model performance, robustness, and sensitivity to rare pathological events.

2. Literature Review and Problem Statement

Electrocardiographic (ECG) signals are a central tool for diagnosing cardiac rhythm and conduction disorders. The diagnostic value of ECG relies not only on the morphology of individual waves but also on subtle variations in their duration, amplitude, wave-front slopes, and interval ratios, which are critical for detecting early stages of arrhythmias and ischemic changes [5, 6]. Preservation of these features depends on high-quality preprocessing, making filtering and normalization stages essential for maintaining diagnostically relevant characteristics [7].

Classical ECG processing methods, developed in the foundational works of Pan and Tompkins (1985), Tompkins (1993), and studies associated with the MIT-BIH Arrhythmia Database (2001), established the basis for QRS complex detection, noise removal, and standardization of analysis approaches [8, 9]. Sörnmo and Laguna further systematized filtering strategies, artifact models, and baseline drift correction techniques [10]. Despite these advances, traditional filters – including low-pass, high-pass, band-pass, and adaptive types – remain limited when applied to real clinical data containing motion artifacts, myogenic noise, sudden baseline shifts, and uneven sampling frequency, particularly in long-term Holter recordings [5, 6].

Adaptive filtering methods, such as LMS- and RLS-based algorithms (Widrow, Haykin), enable real-time spectral adaptation [6]. Kalman filtering and its nonlinear extensions (Extended and Unscented Kalman Filters) have been successfully applied to reconstruct P-waves and suppress biomechanical noise while preserving QRS complex and ST-segment morphology, as illustrated in Figure 1 [5]. Unlike static filters, these approaches reduce the loss of diagnostically critical features, which is especially important for long-duration and noisy recordings [1].

Wavelet transforms have been widely adopted for ECG preprocessing due to their ability to represent signals at multiple scales [7, 11, 12]. Wavelets such as Db4, Db6, or Symlet enable multilevel extraction of the QRS complex, while adaptive thresholding of coefficients suppresses high-frequency noise [11, 12]. Multilevel decomposition with subsequent reconstruction preserves small P-wave components often lost during classical filtering [7].

Statistical and clustering approaches, including Gaussian Mixture Models (GMM), Hidden Markov Models (HMM), DBSCAN, and Spectral Clustering, facilitate grouping of cardiac cycles and identification of pathological rhythm patterns, such as atrial extrasystoles or fibrillation episodes [13, 14]. These methods reduce noise influence and structure large datasets, preparing segments for machine learning models like CNNs, LSTMs, and hybrid architectures [15, 2]. Adaptive clustering combined with dimensionality reduction methods such as UMAP has demonstrated high effectiveness in analyzing large clinical ECG streams [14, 1].

The introduction of deep learning has significantly advanced automated ECG analysis. Classical classifiers (SVM, kNN, naïve Bayes) were limited in capturing complex nonlinear dependencies in

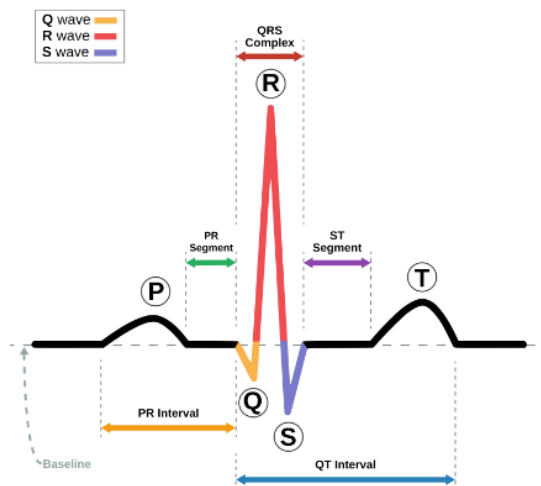


Fig. 1. QRS complex visualization

high-dimensional ECG time series [15, 16]. CNNs efficiently extract local QRS patterns, while LSTM and CNN-LSTM hybrids preserve long-term dependencies [17, 18].

Knowledge-Augmented Networks (KAN) integrate MLP architectures with radial basis functions (RBF), compensating for limitations in modeling local nonlinearities [17, 18, 19]. RBF components allow the network to adapt to variations in individual complexes, reducing dependence on specific patients or recording devices. KAN models show improved arrhythmia recognition on noisy datasets such as MIT-BIH Noise Stress Test Database and real-world clinical streams [17, 20]. Wavelet-based preprocessing further enhances KAN models by providing a multilevel time–frequency representation of ECG segments, preserving local morphology and improving robustness to noise while maintaining computational efficiency [7].

Despite these advances, several challenges remain. Segmentation and normalization parameters strongly influence QRS morphology, amplitude ratios, and temporal intervals, affecting classification accuracy and model stability across different devices and patient populations. Real-world ECG signals often contain electromagnetic interference, motion artifacts, and electrode-related distortions, yet the robustness of modern neural network architectures – including MLP, RBF-KAN, and wavelet-KAN models – under such conditions is insufficiently studied. Comparisons between architectures are necessary to determine which approach best balances artifact resistance, training efficiency, and classification accuracy.

Thus, the present study addresses the following objectives:

- Evaluate the impact of segmentation, normalization, and noise parameters on model performance;
- Compare the effectiveness of MLP, RBF-KAN, and wavelet-KAN models for ECG classification;
- Improve the reliability of automated cardiac diagnostics;
- Develop practical guidelines for model configuration and preprocessing across clinical scenarios.

3. Aim and Objectives of the Study

The aim of this study is the development and systematic evaluation of a KAN-type neural network for ECG signal classification, taking into account the influence of segmentation parameters, normalization methods, and architectural configurations, including RBF and wavelet components. The research focuses on identifying configurations that provide an optimal balance between classification accuracy, the network’s ability to capture local time–frequency patterns of the signal, robustness to noisy data, and training efficiency.

The objectives of the study include:

- preparation of the ECG dataset, including segmentation of signals of varying lengths (100...250 samples), normalization, and class balancing to ensure a stable foundation for model training;
- development and tuning of the baseline MLP model, the MLP-KAN architecture with varying numbers of radial basis functions (RBF: 4, 6, 8), and integration of wavelet preprocessing (MLP-KAN-WT) for subsequent performance comparison;
- analysis of the impact of segmentation and normalization parameters on model accuracy and stability;
- investigation of model effectiveness in detecting rare classes (extrasystoles, class V) through data balancing and F1-score evaluation;
- visualization and assessment of classification results using confusion matrices to compare baseline MLP, MLP-KAN, and MLP-KAN-WT;
- evaluation of model training time to determine the trade-off between computational efficiency and processing speed.

4. Materials And Methods

The study utilized the MIT-BIH Arrhythmia Database [9], a standard dataset for ECG-based arrhythmia classification tasks. This database contains recordings of various cardiac rhythms, allowing modeling of both normal and pathological signals.

Signal segmentation was performed based on R-peaks, as the R-peak represents the most prominent part of the QRS complex, serving as a reliable reference point for defining the start and end of each cardiac cycle. Segmenting by R-peaks standardizes the length of input signal windows, reduces

the impact of interbeat variability, and facilitates the extraction of local morphological ECG features. Figure 1 illustrates an example ECG signal with highlighted R-peaks used for segmentation.

Class labels N (normal rhythm) and V (extrasystoles / premature ventricular contractions) were converted into numeric format to ensure compatibility with machine learning algorithms. Normal rhythm (N) includes QRS complexes without arrhythmic signs, characterized by regular heart rates and stable amplitude-time characteristics. Extrasystoles (V) are premature ventricular beats differing in shape, amplitude, or RR interval. Although rare, these events are clinically significant. This labeling approach enables models to learn normal patterns while simultaneously evaluating their ability to detect pathological signals, which is critical for automated diagnostic applications [21].

The dataset was split into training and testing sets while preserving class proportions to provide representative evaluation of model performance and reduce overfitting risk. To ensure training stability and comparability across different signal segments, data normalization was applied. This preprocessing step scales input features to a uniform range, improving convergence during training and the reliability of performance evaluation.

4.1. Data Preprocessing

Normalization is a critical step for the operation of multilayer perceptrons (MLPs) and KAN-type neural networks, as these models are sensitive to the scale of input data. ECG signals vary in amplitude due to patient-specific characteristics, sensor placement, and recording conditions. Without normalization, larger amplitude signals could dominate the learning process, leading to biased or unstable model behavior.

In this study, each ECG segment $x = [x_1, x_2, \dots, x_n]$ was rescaled to the range $[0,1]$ using min-max normalization:

$$x'_i = \frac{x_i - x_{\min}}{x_{\max} - x_{\min}},$$

where: x is the original signal value, x_{\min} and x_{\max} are the minimum and maximum values of the segment, respectively, and x' is the normalized value [22].

Normalization ensures that models consistently capture both local and global features of ECG signals. It also improves the comparability of results across experiments, reduces training time, and enhances generalization to unseen data, which is particularly important for clinical applications.

In addition to amplitude normalization, the dataset was structured to maintain class balance. Ventricular extrasystoles (class V) are less frequent than normal beats (class N), and an unbalanced dataset can bias the model toward the majority class. The training set was constructed to provide sufficient representation of rare pathological events, ensuring the model learns to detect clinically significant anomalies.

4.2. Model Architectures

The multilayer perceptron (MLP) is a fundamental neural network architecture commonly used for classification tasks due to its ability to model nonlinear relationships between input features and target classes [23]. The network consists of fully connected layers, where each neuron receives input from all neurons of the previous layer, applies learned weights, passes the result through an activation function, and forwards the signal to subsequent layers.

ECG signals were divided into fixed-length windows of 200 samples, each corresponding to an individual cardiac cycle centered on the R-peak. Such segmentation standardizes the input length, reduces interbeat variability, and enables the model to effectively capture both local morphological features and temporal patterns of the QRS complex.

In this study, the MLP processes one-dimensional ECG segments of 200 samples, representing individual cardiac cycles. Input normalization to the $0 \dots 1$ range standardizes amplitudes across different patients and segments, promoting stable training and consistent feature representation [22].

The network comprises two hidden Dense layers. The first layer contains 128 neurons with ReLU activation, responsible for extracting local morphological features of the ECG, including wave peaks, slopes, and the overall shape of the QRS complex. A Dropout layer with 0.2 probability follows to reduce overfitting. The second hidden Dense layer has 64 neurons, also with ReLU activation, and is followed by a Dropout layer with 0.1 probability for additional regularization.

The output layer consists of two neurons corresponding to N (normal rhythm) and V (ventricular extrasystoles) classes, with a Softmax activation function to generate class probabilities:

$$P(y = i) = \frac{e^{z_i}}{\sum_j e^{z_j}},$$

where: z_i represents the linear combination of weighted inputs for the i -th output neuron.

Figure 2 presents the schematic of the MLP architecture, showing the sequential processing of ECG segments from input normalization through hidden layers to class probability outputs. The design ensures comprehensive capture of local and global morphological features for accurate classification of normal and pathological cardiac events.

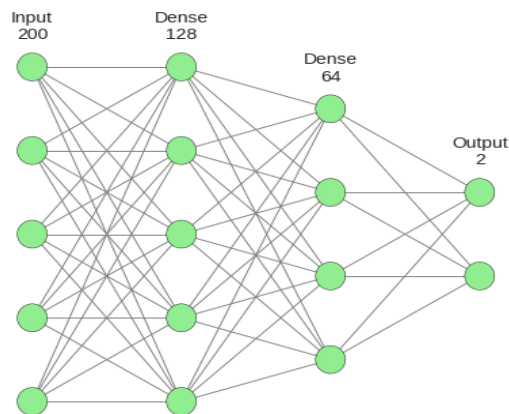


Fig. 2. Schematic of basic MLP

The MLP-KAN (Knowledge-Augmented Network) model represents an extension of the classical multilayer perceptron through the integration of a KAN layer [24]. This layer enhances the network’s ability to capture local variations and subtle morphological patterns in ECG signals, which are often critical for detecting rare or irregular events. The KAN layer incorporates radial basis functions (RBFs) to supplement the fully connected structure of the MLP, enabling the modeling of complex nonlinear relationships that standard dense layers alone may not adequately represent [25].

The input layer processes normalized ECG segments of 200 samples, consistent with the baseline MLP [26]. Within the KAN layer, each neuron corresponds to a Gaussian RBF, and in this study, four RBF units are used to capture localized morphological features. These functions generate selective responses to specific ECG characteristics, such as sharp peaks or deviations in wave slopes, increasing the network’s sensitivity to clinically significant variations [27]. The output of the i -th RBF neuron is defined as:

$$\varphi_i(x) = \exp\left(-\frac{(x - c_i)^2}{2\sigma^2}\right),$$

where: x is the input segment value, c_i is the center of the i -th RBF, and σ is the width parameter controlling the locality of the function’s influence [28, 29, 30]. Figure 3 illustrates the four Gaussian RBF functions applied to a representative ECG segment, with each function labeled $\varphi_0, \varphi_1, \varphi_2, \varphi_3$.

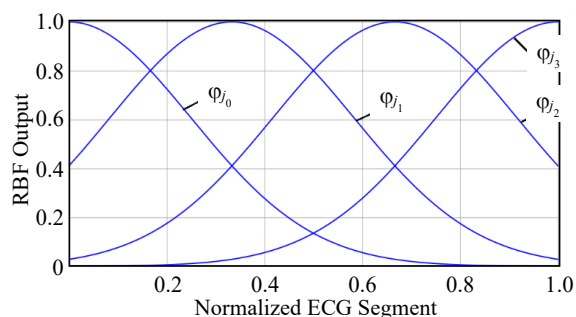


Fig. 3. Typical form of functions φ_i for $m = 4$

The outputs of the RBF neurons are then fed into a fully connected Dense layer, where each output is combined with trainable weights optimized during training [31]. This produces a condensed representation of the local morphological features detected by the RBFs. Subsequently, the representation is processed through two hidden Dense layers with 128 and 64 neurons, applying ReLU activation and Dropout regularization to enhance feature integration, nonlinearity, and generalization [32].

Finally, the output Dense layer contains two neurons with a Softmax activation function, yielding probabilities for classification into N (normal rhythm) and V (extrasystoles). This layered organization allows the network to combine localized feature extraction via RBFs with global pattern integration, ensuring that subtle variations in ECG signals, including rare or irregular events, contribute effectively to the classification decision.

The overall MLP-KAN architecture, showing the RBF layer in parallel with the fully connected hidden layers and the final output layer, is presented in Figure 4. This schematic highlights how local signal characteristics are extracted and integrated to improve classification performance on both typical and atypical ECG patterns.

The MLP-KAN-WT (Multilayer Perceptron with Knowledge-Augmented and Wavelet Transform) model extends the classical MLP-KAN architecture by replacing the radial basis functions in the KAN lay-

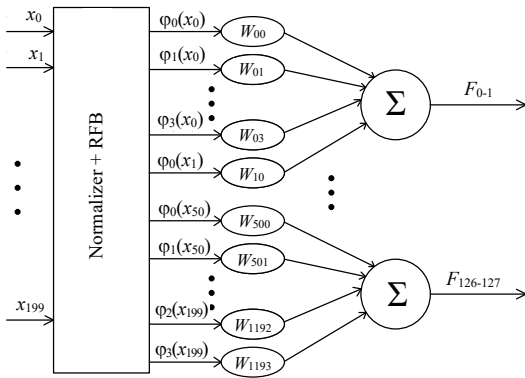


Fig. 4. Example of KAN layer

(level 4), Symlet 4 (level 4), and Coiflet 5 (level 5), providing diverse basis functions capable of representing a range of ECG signal characteristics. Each wavelet function $\psi_j(t)$ transforms the input segment $x(t)$ into a feature representation:

$$\phi_j(x) = \sum_{t=1}^n x(t) \cdot \psi_j(t),$$

where: n is the number of samples in the segment. The trainable parameters of each wavelet allow the network to adapt to variations in signal morphology and inter-patient differences.

The outputs of the wavelet functions are subsequently fed into two fully connected Dense layers for feature integration. The first Dense layer contains 128 neurons with ReLU activation and a Dropout probability of 0.2, while the second layer has 64 neurons with ReLU and Dropout 0.1. This structure aggregates the extracted time-frequency features, introduces nonlinearity, and supports stable model training.

Figure 5 illustrates the typical forms of the five shifted Daubechies 4 wavelet functions applied to a representative ECG segment. The graph demonstrates how these wavelets localize and detect subtle signal variations. Figure 6 presents the complete schematic of the MLP-KAN-WT architecture, showing the integration of the KAN-Wavelet layer with the subsequent Dense layers and output classification layer. This architecture ensures effective extraction of local and time–frequency features, increases robustness to noise and inter-patient variability, and improves arrhythmia classification accuracy compared to the classical MLP-KAN model.

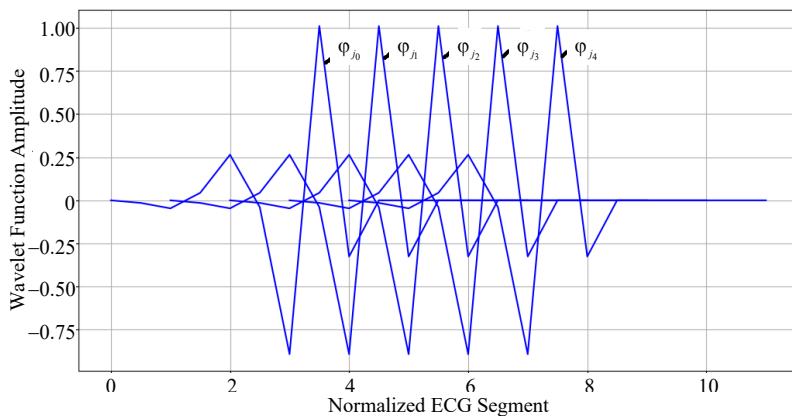


Fig. 5. Typical form of wavelet functions Daubechies 4 ϕ_j for $m = 5$

4.3. Experiments

The experimental part of the study focused on a comprehensive evaluation of three distinct architectures: the baseline MLP, the MLP-KAN model incorporating a kernel layer for local nonlinear approximation, and the modified MLP-KAN-WT, which combines the KAN approach with multiscale features ob-

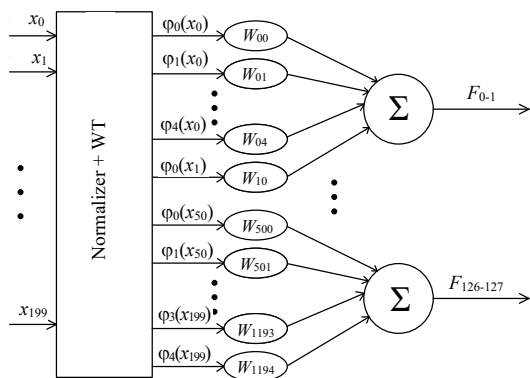


Fig. 6. Examzple of KAN layer with WT

tained through discrete wavelet transforms. For MLP-KAN-WT, Haar wavelets with decomposition level 1, Daubechies 4 with level 4, Symlet 4 with level 4, and Coiflet 5 with level 5 were selected.

The choice of decomposition levels was guided by energy and entropy criteria as proposed in [7, 33]. Signal energy reflects the concentration of information at a particular scale, while entropy measures the disorder of the coefficients. Selecting levels that maximize energy and minimize entropy allows automatic identification of scales that best capture both local and frequency characteristics of ECG signals.

All models were trained under a unified optimization scheme using the Adam optimizer with a learning rate of 0.001, fixed-size mini-batches, and categorical cross-entropy as the loss function. Initial weights were identical across runs to minimize variability and allow

reliable statistical comparison. Evaluation was performed on an independent test set, recording performance metrics such as overall accuracy, class-specific $F1$ -score, precision, recall, and training time.

A substantial portion of the experiments examined the impact of input window size. ECG signals were divided into fixed-length segments of 200 samples, corresponding to individual cardiac cycles centered on the R-peak. This interval provides sufficient morphological information to capture characteristic QRS features while reducing interbeat variability. Additional segment lengths of 100, 150, and 250 samples were tested to assess sensitivity to available temporal context.

Class imbalance was explicitly addressed: the dataset contained a majority of normal beats (class N) and a relative scarcity of ventricular ectopic beats (class V). Oversampling of class V was applied during training to ensure sufficient representation, mitigating bias toward the dominant class and enabling accurate evaluation of models' ability to detect clinically relevant anomalies.

For MLP-KAN, the capacity of the kernel layer was varied by adjusting the number of radial basis functions (4, 6, or 8 RBF) to evaluate the effect of increased nonlinear space complexity on the detection of subtle morphological changes. In MLP-KAN-WT, wavelet transforms represent ECG signals across multiple levels, preserving local variations such as short impulses, abrupt transitions, and fine-grained features that conventional dense layers or RBFs may smooth out.

Learning curves illustrating loss and accuracy on training and validation sets were generated for all architectures. These curves provide insight into convergence speed, stability, and the influence of the KAN layer and wavelet-based feature extraction on regularization and generalization. Figure 7 presents the loss curves, while Figure 8 shows accuracy progression.

Confusion matrices were analyzed in detail to reveal characteristic misclassifications, such as ventricular ectopic beats labeled as normal. These patterns highlight how the integration of local nonlinear processing in the KAN layer and multiscale wavelet features in MLP-KAN-WT improve recognition of complex morphological structures.

Overall, these experiments provide a holistic understanding of the functional advantages and limitations of each model, demonstrating how architectural choices, input segmentation, and class

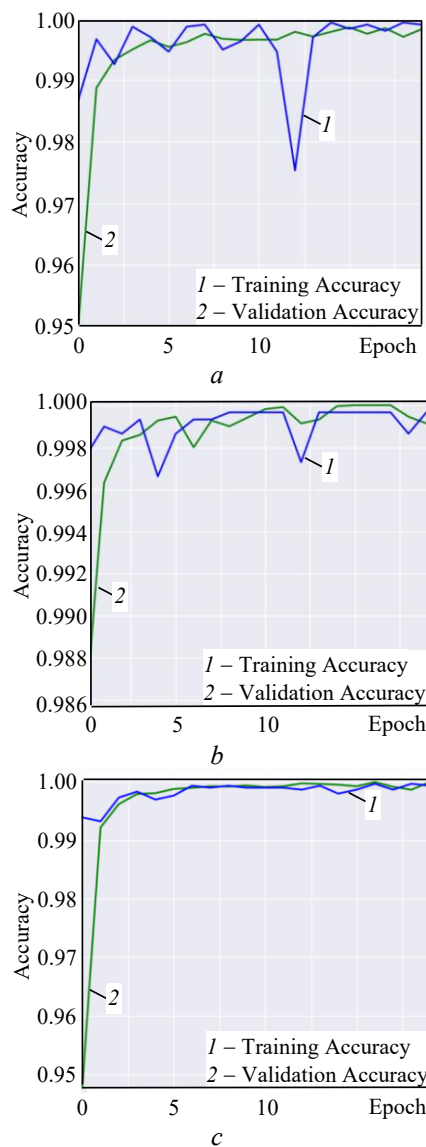


Fig. 7. Learning curves: a – for MLP; b – for MLP-KAN; c – for MLP-KAN-WT, showing both training and validation loss and accuracy over epochs

balancing influence classification performance, robustness to noisy or variable signals, and computational efficiency.

5. Research Results

The evaluation of the baseline MLP and its KAN-augmented variants was performed using three primary metrics: overall classification accuracy, $F1$ -score for class V (ventricular ectopic beats), and training time. Given that class V occurs far less frequently than class N (normal rhythm), the $F1$ -score serves as a critical measure of the model's ability to correctly identify rare pathological segments. Training time provides insight into computational efficiency and highlights the trade-off between learning speed and classification performance, which is especially important in real-time clinical scenarios.

All models were trained on normalized ECG segments of 200 samples each, scaled to the $[0,1]$ range. Normalization ensures uniform signal amplitude across different patients and segments, promoting stable training and consistent feature representation. To mitigate class imbalance, additional class V segments from multiple records in the MIT-BIH dataset were included, ensuring a representative number of examples for both classes and reducing overfitting toward the dominant class N . Specifically, the training set contained approximately 90% class N and 10% class V segments, reflecting the natural prevalence of these rhythms while providing sufficient samples for robust learning of rare events.

Test results, summarized in Table 1, show the performance of the baseline MLP, the MLP-KAN models with RBF layers, and the MLP-KAN-WT variants using wavelet preprocessing. The data indicate that the integration of a KAN layer and wavelet transforms improves both overall classification accuracy and the $F1$ -score for the underrepresented class V compared to the standard MLP. This confirms the advantages of combining local nonlinear modeling with multiscale time-frequency feature extraction.

The baseline MLP achieved an overall accuracy of 0.9993, but its ability to detect rare class V segments was limited, as reflected by an $F1$ -score of 0.9951. The addition of the KAN layer with 8 RBF units (MLP-KAN-RBF8) increased the $F1$ -score to 0.9976, at the expense of higher training time (61.07 s). The MLP-KAN-WT model with Haar wavelet preprocessing (level 1) achieved a comparable $F1$ -score of 0.9976 while maintaining lower computational cost (41.46 s), demonstrating that wavelet preprocessing efficiently enhances detection of rare pathological events without compromising performance for the main class N :

$$F1\text{-score} = 2 \cdot \frac{\text{Precision} \cdot \text{Recall}}{\text{Precision} + \text{Recall}},$$

$$\text{Precision} = \frac{TP}{TP + FP}, \text{Recall} = \frac{TP}{TP + FN},$$

where: TP, FP, and FN represent true positives, false positives, and false negatives for class V , respectively.

Table 1

Comparative Results

Model	Accuracy	$F1$ V	Precision V	Recall V	Time s
MLP	0.999324	0.995146	0.990338	1.000000	32.36
MLP-KAN-RBF4	0.999324	0.995146	0.990338	1.000000	46.12
MLP-KAN-RBF6	0.999324	0.995122	0.995122	0.995122	66.43
MLP-KAN-RBF8	0.999662	0.997555	1.000000	0.995122	61.07
MLP-KAN-WT-haar 1	0.999662	0.997555	1.000000	0.995122	41.46
MLP-KAN-WT-db4 4	0.998648	0.990243	0.990243	0.990243	43.24
MLP-KAN-WT-sym 4	0.998648	0.990243	0.990243	0.990243	52.01
MLP-KAN-WT-coif 5	0.998648	0.990148	0.990148	0.990148	51.64

Training dynamics were assessed through learning curves for each model, showing both accuracy and loss over epochs (Figure 8). These curves confirm that the baseline MLP quickly reaches high accuracy but exhibits fluctuations late in training, indicating some instability in detecting class V . In contrast, the modified architectures with KAN and wavelet preprocessing exhibit smoother, more stable learning, maintaining peak accuracy around 0.9997:

$$\text{Accuracy} = \frac{\text{TP} + \text{TN}}{\text{TP} + \text{TN} + \text{FP} + \text{FN}}$$

Confusion matrices further illustrate model performance. For the MLP-KAN-RBF8 model (Figure 9), class *N* achieved 2,743 correct predictions with 10 misclassified as class *V*, while class *V* had 189 correct predictions with 16 misclassified as class *N*. For the MLP-KAN-WT with Haar wavelet preprocessing (Figure 10), class *N* had 2,754 correct predictions with zero misclassifications, and class *V* had 204 correct predictions with only 7 misclassifications. These results highlight the improved sensitivity and stability provided by wavelet preprocessing combined with the KAN layer.

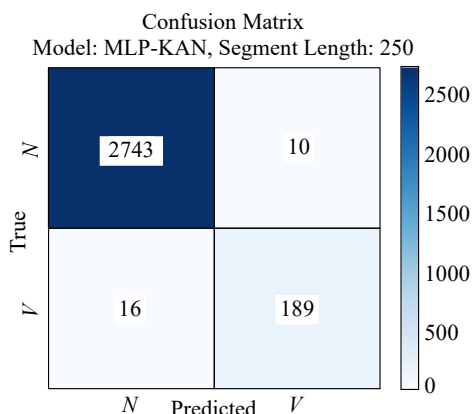


Fig. 8. Confusion Matrix: MLP-KAN- RBF8

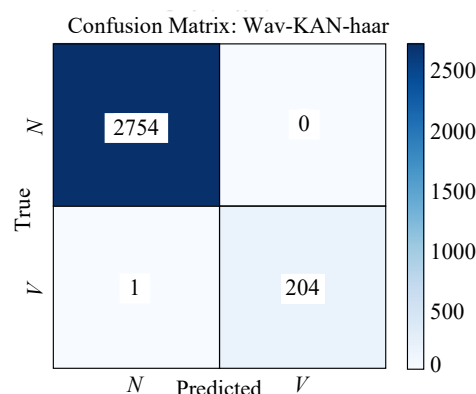


Fig. 9. Confusion Matrix: MLP -KAN-WT-haar_1

6. Conclusions

The experiments demonstrated that integrating the KAN layer into the baseline MLP architecture significantly improves ECG segment classification accuracy. The baseline MLP achieved an accuracy of 0.9993, whereas the modified MLP-KAN-RBF8 reached 0.9997, with the *F1*-score for the rare class *V* increasing from 0.9951 to 0.9976.

The model with Haar wavelet preprocessing— MLP-KAN-WT (Haar wavelet, level 1) – achieved comparable results: accuracy of 0.9997 and *F1*-score for class *V* of 0.9976, with relatively lower computational costs. This indicates that wavelet preprocessing maintains high model performance while reducing training time.

MLP-KAN exhibited higher training stability and better robustness to segment variations. Validation accuracy for the modified models remained at 0.9997, whereas the baseline MLP showed larger fluctuations in later epochs. Increasing the number of RBFs from 4 to 8 improved classification accuracy for class *V* by approximately 0.2...0.3 %, although training time increased by 32...35 s. Wavelet preprocessing ensures an optimal balance between high accuracy and computational efficiency.

Analysis of confusion matrices confirmed that MLP-KAN substantially reduces misclassifications of class *V* segments compared to the baseline MLP while maintaining high accuracy for class *N*. Overall results indicate model stability and effective capture of local nonlinearities in the signal, enhancing generalization on test data.

These findings support the use of the KAN layer for automated ECG classification tasks, providing a balance between accuracy, *F1*-score, and computational cost, making this approach promising for practical medical applications. Using wavelet preprocessing, as in the MLP-KAN-WT model with Haar wavelet (level 1), achieves high performance at an optimal computational complexity.

Thus, combining wavelet preprocessing with the KAN layer offers the best compromise between classification accuracy, sensitivity to rare segments, and computational efficiency, making this approach particularly suitable for practical automated ECG analysis.

Література

1. Hemanth D. J., Gupta D., Balas V. E. Intelligent Data Analysis for Biomedical Applications. Academic Press, 2019. 420 p. DOI: <https://doi.org/10.1016/C2017-0-03676-5>.
2. Deep learning-based ECG arrhythmia classification: A systematic review / Q. Xiao et al. *Applied Sciences*. 2023. Vol. 13, Issue 8. Art. 4964. DOI: <https://doi.org/10.3390/app13084964>.

3. The applications of deep learning in ECG classification for disease diagnosis: A systematic review and meta-data analysis / M. Khalid et al. *Engineering Journal*. 2024. Vol. 28, Issue 8. P. 45–77. DOI: <https://doi.org/10.4186/ej.2024.28.8.45>.
4. MLP-K AN: implementation of the Kolmogorov-Arnold layer in a multilayer perceptron / O. Galchonkov et al. *Eastern-European Journal of Enterprise Technologies*. 2025. Vol. 3/4 (135). P. 34–41. DOI: <https://doi.org/10.15587/1729-4061.2025.328928>.
5. Ahmed A. F., Al-Obaidi M. K. A review of ECG signal filtering approaches. *Global Journal of Engineering and Technology Advances*. 2022. Vol. 11, Issue 3. P. 093–097. DOI: <https://doi.org/10.30574/gjeta.2022.11.3.0099>.
6. Sharma N., Sidhu J. S. Removal of noise from ECG signal using adaptive filtering. *Indian Journal of Science and Technology*. 2016. Vol. 9 (48). DOI: <https://doi.org/10.17485/ijst/2016/v9i48/106424>.
7. Shcherbakova G., Koshutina D. Development of a criterion for selecting the level of wavelet decomposition for QRS detection in electrocardiogram signals using energy and entropy. *Proceedings of Odessa Polytechnic University*. 2025. Issue 1 (71). P. 157–166. DOI: <https://doi.org/10.15276/opu.1.71.2025.18>.
8. Pan J., Tompkins W. J. A Real-Time QRS Detection Algorithm. *IEEE Transactions on Biomedical Engineering*. 1985. Vol. BME-32, Issue 3. P. 230–236. DOI: 10.1109/TBME.1985.325532.
9. MIT-BIH Arrhythmia Database / PhysioNet. URL: <https://www.physionet.org/content/mitdb/1.0.0/> (дата звернення: 16.11.2025).
10. Sörnmo L., Laguna P. *Electrocardiogram Signal Processing*, Wiley, 2005. 680 p.
11. He H., Tan Y., Wang Y. Optimal base wavelet selection for ECG noise reduction using a comprehensive entropy criterion. *Entropy*. 2015. Vol. 17, Issue 9. P. 6093–6109. DOI: <https://doi.org/10.3390/e17096093>.
12. Agrawal P., Arun V., Basu A. Artificial Neural Network Based ECG Feature Extraction Using Wavelet Transform. *Emerging Wireless Technologies and Sciences. ICEWTS 2024*. Cham: Springer, 2025. P. 8–22. (CCIS; vol. 2399). DOI: https://doi.org/10.1007/978-3-031-87886-2_2.
13. Scalable clustering of complex ECG health data: Big data clustering analysis with UMAP and HDBSCAN / V. Kaverinskiy et al. *Computation*. 2025. Vol. 13, Issue 6. Art. 144. DOI: <https://doi.org/10.3390/computation13060144>.
14. Adaptive clustering for distribution parameter estimation in technical diagnostics / G. Shcherbakova et al. *12th International Conference on Applied Innovations in IT (ICAIIIT)*, Köthen, Germany, 2024. DOI: <https://doi.org/10.25673/115650>.
15. ECG analysis using consensus clustering / A. Lourenço et al. *2014 22nd European Signal Processing Conference (EUSIPCO)*, Lisbon, Portugal, 2014. P. 511–515.
16. Evaluating binary classifiers for cardiovascular disease prediction: Enhancing early diagnostic capabilities / P. Iacobescu et al. *Journal of Cardiovascular Development and Disease (JCDD)*. 2024. Vol. 11, Issue 12. Art. 396. DOI: <https://doi.org/10.3390/jcdd11120396>.
17. Guo C., Ahmed S., Alouini M.-S. Machine learning-based automatic cardiovascular disease diagnosis using two ECG leads. 2023. DOI: <https://doi.org/10.48550/arXiv.2305.16055>.
18. Wu Z., Guo C. Deep learning and electrocardiography: Systematic review of current techniques in cardiovascular disease diagnosis and management. *BioMed Eng OnLine*. 2025. Vol. 24. Art. 23. DOI: <https://doi.org/10.1186/s12938-025-01349-w>.
19. Savalia S., Emamian V. Cardiac arrhythmia classification by multi-layer perceptron and convolution neural networks. *Bioengineering*. 2018. Vol. 5, Issue 2. Art. 35. DOI: <https://doi.org/10.3390/bioengineering5020035>.
20. Li Z. Kolmogorov-Arnold networks are radial basis function networks. 2024. arXiv:2405.06721. URL: <https://arxiv.org/abs/2405.06721>.
21. Classification of arrhythmia based on convolutional neural networks and encoder-decoder model / J. Liu et al. *Computer Systems Science and Engineering*. 2022. DOI: <https://doi.org/10.32604/cmc.2022.029227>.
22. Mavaddati S. ECG arrhythmias classification based on deep learning methods and transfer learning technique. *Biomedical Signal Processing and Control*. 2024. DOI: <https://doi.org/10.1016/j.bspc.2024.107236>.
23. Multi-layer perceptron-based data-driven multiscale modelling of granular materials with a novel Frobenius norm-based internal variable / M. Wang et al. *Journal of Rock Mechanics and Geotechnical Engineering*. 2024. DOI: <https://doi.org/10.1016/j.jrmge.2024.02.003>.
24. Hadj Kilani B. Kolmogorov-Arnold networks: Key developments and uses. 2024. DOI: <https://doi.org/10.32388/7NNCAA>.
25. Yu R., Yu W., Wang X. KAN or MLP: A fairer comparison. 2024. DOI: <https://doi.org/10.48550/arXiv.2407.16674>.

26. KAN: Kolmogorov-Arnold Networks / Z. Liu et al. 2024. arXiv:2404.19656. URL: <https://arxiv.org/abs/2404.19756>.
27. Ismayilova A., Ismayilov M. On the universal approximation property of radial basis function neural networks. 2023. arXiv:2304.02220. URL: <https://arxiv.org/abs/2304.02220>.
28. Ta T. H. BSRBF-KAN: A combination of B-splines and radial basis functions in Kolmogorov-Arnold networks. 2024. DOI: <https://doi.org/10.13140/RG.2.2.16755.54562>.
29. Hollósi J. Efficiency analysis of Kolmogorov–Arnold networks for visual data processing. *SMTS 2024 Conference Proceedings*. 2024. DOI: <https://doi.org/10.3390/engproc2024079068>.
30. Seghouane A.-K., Shokouhi N. Adaptive learning for robust radial basis function networks. *IEEE Transactions on Cybernetics*. 2021. Vol. 51, Issue 5. P. 2847–2856. DOI: <https://doi.org/10.1109/TCYB.2019.2951811>.
31. Panda S., Panda G. On the development and performance evaluation of improved radial basis function neural networks. *IEEE Transactions on Systems, Man, and Cybernetics: Systems*. 2022. Vol. 52, Issue 6. P. 3873–3884. DOI: <https://doi.org/10.1109/TSMC.2021.3076747>.
32. Bozorgasl Z., Chen H. Wav-KAN: Wavelet Kolmogorov-Arnold networks. 2024. arXiv:2405.12832. URL: <https://arxiv.org/abs/2405.12832>.
33. Koshutina D. V., Shcherbakova H. Yu. Automated selection of wavelet decomposition level based on energy and entropy for QRS complex detection in ECG. *Modern Information Technologies – 2025: proc. 15th Int. Sci. Conf. for Students and Young Scientists*, Odessa, Ukraine, May 15–16, 2025. Odessa: Nauka i Tekhnika, 2025. P. 21–23. DOI: <https://doi.org/10.5281/zenodo.15521809>.

References

1. Hemanth, D. J., Gupta, D., & Balas, V. E. (2019). *Intelligent data analysis for biomedical applications*. Academic Press. DOI: <https://doi.org/10.1016/C2017-0-03676-5>.
2. Xiao, Q., Lee, K., Mokhtar, S. A., Ismail, I., Md Pauzi, A. L., Zhang, Q., & Lim, P. Y. (2023). Deep learning-based ECG arrhythmia classification: A systematic review. *Applied Sciences*, 13(8), Article 4964. DOI: <https://doi.org/10.3390/app13084964>.
3. Khalid, M., Pluempitiwiriyawej, C., Wangsiripitak, S., & Abdulkadhem, A. A. (2024). The applications of deep learning in ECG classification for disease diagnosis: A systematic review and meta-data analysis. *Engineering Journal*, 28(8), 45–77. DOI: <https://doi.org/10.4186/ej.2024.28.8.45>.
4. Galchonkov, O., Baranov, O., Maslov, O., Babych, M., & Baskov, I. (2025). MLP-K AN: Implementation of the Kolmogorov-Arnold layer in a multilayer perceptron. *Eastern-European Journal of Enterprise Technologies*, 3/4(135), 34–41. DOI: <https://doi.org/10.15587/1729-4061.2025.328928>.
5. Ahmed, A. F., & Al-Obaidi, M. K. (2022). A review of ECG signal filtering approaches. *Global Journal of Engineering and Technology Advances*, 11(3), 093–097. DOI: <https://doi.org/10.30574/gjeta.2022.11.3.0099>.
6. Sharma, N., & Sidhu, J. S. (2016). Removal of noise from ECG signal using adaptive filtering. *Indian Journal of Science and Technology*, 9(48). DOI: <https://doi.org/10.17485/ijst/2016/v9i48/106424>.
7. Shcherbakova, G., & Koshutina, D. (2025). Development of a criterion for selecting the level of wavelet decomposition for QRS detection in electrocardiogram signals using energy and entropy. *Proceedings of Odessa Polytechnic University*, 1(71), 157–166. DOI: <https://doi.org/10.15276/opu.1.71.2025.18>.
8. Pan, J., & Tompkins, W. J. (1985). A real-time QRS detection algorithm. *IEEE Transactions on Biomedical Engineering*, BME-32(3), 230–236. DOI: 10.1109/TBME.1985.325532.
9. PhysioNet. (n.d.). *MIT-BIH Arrhythmia Database*. Retrieved from <https://www.physionet.org/content/mitdb/1.0.0>.
10. Sörnmo, L., & Laguna, P. (2005). *Electrocardiogram signal processing*. Wiley.
11. He, H., Tan, Y., & Wang, Y. (2015). Optimal base wavelet selection for ECG noise reduction using a comprehensive entropy criterion. *Entropy*, 17(9), 6093–6109. DOI: <https://doi.org/10.3390/e17096093>.
12. Agrawal, P., Arun, V., & Basu, A. (2025). Artificial neural network based ECG feature extraction using wavelet transform. In *Emerging Wireless Technologies and Sciences. ICEWTS 2024* (CCIS, Vol. 2399, pp. 8–22). Springer, Cham. DOI: https://doi.org/10.1007/978-3-031-87886-2_2.
13. Kaverinskiy, V., Chaikovskiy, I., Mnevets, A., & Malakhov, K. S. (2025). Scalable clustering of complex ECG health data: Big data clustering analysis with UMAP and HDBSCAN. *Computation*, 13(6), Article 144. DOI: <https://doi.org/10.3390/computation13060144>.
14. Shcherbakova, G., Antoshchuk, S., Koshutina, D., & Sakhno, K. (2024). Adaptive clustering for distribution parameter estimation in technical diagnostics. *12th International Conference on Applied Innovations in IT (ICAIIIT)*, Köthen, Germany. DOI: <https://doi.org/10.25673/115650>.

15. Lourenço, A., Carreiras, C., Bulò, S. R., & Fred, A. (2014, August 25–29). *ECG analysis using consensus clustering* [Paper presentation]. 2014 22nd European Signal Processing Conference (EUSIPCO), Lisbon, Portugal.
16. Iacobescu, P., Marina, V., Anghel, C., & Anghel, A. (2024). Evaluating binary classifiers for cardiovascular disease prediction: Enhancing early diagnostic capabilities. *Journal of Cardiovascular Development and Disease (JCDD)*, 11(12), Article 396. DOI: <https://doi.org/10.3390/jcdd11120396>.
17. Guo, C., Ahmed, S., & Alouini, M.-S. (2023). *Machine learning-based automatic cardiovascular disease diagnosis using two ECG leads*. arXiv. DOI: <https://doi.org/10.48550/arXiv.2305.16055>.
18. Wu, Z., & Guo, C. (2025). Deep learning and electrocardiography: Systematic review of current techniques in cardiovascular disease diagnosis and management. *BioMed Eng OnLine*, 24, Article 23. DOI: <https://doi.org/10.1186/s12938-025-01349-w>.
19. Savalia, S., & Emamian, V. (2018). Cardiac arrhythmia classification by multi-layer perceptron and convolution neural networks. *Bioengineering*, 5(2), Article 35. DOI: <https://doi.org/10.3390/bioengineering5020035>.
20. Li, Z. (2024). *Kolmogorov-Arnold networks are radial basis function networks*. arXiv. Retrieved from <https://arxiv.org/abs/2405.06721>.
21. Liu, J., Xia, X., Han, C., Hui, J., & Feng, J. (2022). Classification of arrhythmia based on convolutional neural networks and encoder-decoder model. *Computer Systems Science and Engineering*. DOI: <https://doi.org/10.32604/cmc.2022.029227>.
22. Mavaddati, S. (2024). ECG arrhythmias classification based on deep learning methods and transfer learning technique. *Biomedical Signal Processing and Control*. DOI: <https://doi.org/10.1016/j.bspc.2024.107236>.
23. Wang, M., Feng, Y. T., Guan, S., & Qu, T. (2024). Multi-layer perceptron-based data-driven multiscale modelling of granular materials with a novel Frobenius norm-based internal variable. *Journal of Rock Mechanics and Geotechnical Engineering*. DOI: <https://doi.org/10.1016/j.jrmge.2024.02.003>.
24. Hadj Kilani, B. (2024). *Kolmogorov-Arnold networks: Key developments and uses*. Qeios. DOI: <https://doi.org/10.32388/7NNCAA>.
25. Yu, R., Yu, W., & Wang, X. (2024). *KAN or MLP: A fairer comparison*. arXiv. DOI: <https://doi.org/10.48550/arXiv.2407.16674>.
26. Liu, Z., Wang, Y., Vaidya, S., Ruehle, F., Halverson, J., Soljačić, M., Hou, T. Y., & Tegmark, M. (2024). *KAN: Kolmogorov-Arnold Networks*. arXiv. Retrieved from <https://arxiv.org/abs/2404.19756>.
27. Ismayilova, A., & Ismayilov, M. (2023). *On the universal approximation property of radial basis function neural networks*. arXiv. Retrieved from <https://arxiv.org/abs/2304.02220>.
28. Ta, T. H. (2024). *BSRBF-KAN: A combination of B-splines and radial basis functions in Kolmogorov-Arnold networks*. ResearchGate. DOI: <https://doi.org/10.13140/RG.2.2.16755.54562>.
29. Hollósi, J. (2024). Efficiency analysis of Kolmogorov-Arnold networks for visual data processing. *SMTS 2024 Conference Proceedings*. DOI: <https://doi.org/10.3390/engproc2024079068>.
30. Seghouane, A.-K., & Shokouhi, N. (2021). Adaptive learning for robust radial basis function networks. *IEEE Transactions on Cybernetics*, 51(5), 2847–2856. DOI: <https://doi.org/10.1109/TCYB.2019.2951811>.
31. Panda, S., & Panda, G. (2022). On the development and performance evaluation of improved radial basis function neural networks. *IEEE Transactions on Systems, Man, and Cybernetics: Systems*, 52(6), 3873–3884. DOI: <https://doi.org/10.1109/TSMC.2021.3076747>.
32. Bozorgasl, Z., & Chen, H. (2024). *Wav-KAN: Wavelet Kolmogorov-Arnold networks*. arXiv. Retrieved from <https://arxiv.org/abs/2405.12832>.
33. Koshutina, D. V., & Shcherbakova, H. Y. (2025, May 15–16). *Automated selection of wavelet decomposition level based on energy and entropy for QRS complex detection in ECG* [Paper presentation]. 15th International Scientific Conference for Students and Young Scientists "Modern Information Technologies – 2025", Odesa, Ukraine. DOI: <https://doi.org/10.5281/zenodo.15521809>.

Кошутіна Дар'я Валеріївна; Daria Koshutina ORCID: <https://orcid.org/0009-0004-1326-8775>

Received November 17, 2025

Accepted December 15, 2025